

Duality and integer quantum Hall effect in isotropic 3D crystals

M. Koshino, H. Aoki

Department of Physics, University of Tokyo, Hongo, Tokyo 113-0033, Japan

(October 22, 2018)

We show here a series of energy gaps as in Hofstadter's butterfly, which have been shown to exist by Koshino et al [Phys. Rev. Lett. **86**, 1062 (2001)] for anisotropic three-dimensional (3D) periodic systems in magnetic fields \mathbf{B} , also arise in the isotropic case unless \mathbf{B} points in high-symmetry directions. Accompanying integer quantum Hall conductivities $(\sigma_{xy}, \sigma_{yz}, \sigma_{zx})$ can, surprisingly, take values $\propto (1, 0, 0), (0, 1, 0), (0, 0, 1)$ even for a fixed direction of \mathbf{B} unlike in the anisotropic case. We can intuitively explain the high-magnetic field spectra and the 3D QHE in terms of quantum mechanical hopping by introducing a “duality”, which connects the 3D system in a strong \mathbf{B} with another problem in a weak magnetic field ($\propto 1/B$).

I. INTRODUCTION

Appearance of energy gaps in three-dimensional(3D) systems is a hallmark of quantum mechanics in crystals. There, a periodicity, be it atomic or density-wave formation from some mechanism, gives rise to a Bragg's reflection accompanied by energy gaps as Bloch's theorem dictates. Apart from this, there are few occurrences of energy gaps in 3D (unless of course non-perturbative, many-body states such as the BCS state are involved).

In two-dimensional(2D) systems, by contrast, we do have a remarkable realization of gaps when a magnetic field is applied. For a free 2D electron gas the spectrum even coalesces into a series of sharp Landau levels. When the 2D system has some periodicity (thought of as arising from a periodic potential or tight-binding array of atoms), application of a magnetic field gives rise to a fractal energy gaps, which is called “Hofstadter's butterfly”¹. One way to realize why the butterfly appears is that the two quantizations, one being Bloch's band structure and the other the Landau quantization, interfere with each other. The interference should occur when the band gap, $\hbar^2/(ma^2)$ (m : electron mass, a : lattice constant), and the cyclotron energy, $\hbar\omega_c$, are similar, which indeed amounts to the condition for the appearance of the butterfly, $\phi \sim \phi_0$, where ϕ is the magnetic flux penetrating a unit cell and $\phi_0 = h/e$ the flux quantum.

Once we have an energy gap in a 2D system it is known that the integer quantum Hall effect (IQHE) should occur. Thouless *et al*² in fact have derived a general formula for the quantized Hall conductance in 2D periodic systems without any assumption on the periodicity, and shown that the Hall conductance can be written in terms of some topological invariants.

A natural question is whether we can extend such arguments to 3D systems. It has been shown that, if an energy gap exists in 3D, it should accompany an IQHE where each component of the Hall tensor σ_{ij} is quantized^{3–6}. A big question, then, is whether and how gaps can appear in 3D. We have previously shown that the butterfly-like spectrum indeed appears in *anisotropic* 3D (quasi-1D) lattice and have derived the quantized Hall tensor for each gap.¹² For the anisotropic case we

can intuitively understand these in terms of a mapping between the 3D case and a 2D case. For the isotropic case, however, it seems difficult to have the energy gaps since the magnetic subbands are likely to be overlapped by the large dispersion along the magnetic field. Several authors^{7,8} have computed the energy spectra of the isotropic 3D tight-binding system under magnetic fields pointing to high-symmetry crystallographic directions, and Kunszt⁸ concluded that there is in general no energy gaps although the possibility of gaps cannot be excluded. So the existence of gaps and IQHE remains an open question.

In this paper, we show that we do have energy gaps in *isotropic* 3D lattices rather universally in that all we have to have is the sufficiently large magnetic field \mathbf{B} pointing to general directions (i.e., off the high-symmetry axes). We first show this by calculating energy spectra for various directions of \mathbf{B} . We have also calculated the Hall tensors, $\sigma_{xy}, \sigma_{yz}, \sigma_{zx}$, when the Fermi energy is in each energy gap. They turn out to have values, e.g. $(1, 0, 0), (0, 1, 0), (0, 0, 1)$ in an appropriate unit, even for a fixed direction of \mathbf{B} , which is surprising and unlike in the anisotropic case.

We then intuitively explain such structures in the spectra by introducing a “duality”, which connects the 3D system in a strong \mathbf{B} with another problem in a weak magnetic field ($\sim 1/B$). This enable us to regard the band structure and the quantization of the 3D Hall conductivity as graphically arising from quantum mechanical hopping between “semiclassical” orbits in the weak- B case.

II. FORMULATION OF 3D BLOCH ELECTRONS IN MAGNETIC FIELDS

We take a non-interacting tight-binding model in a uniform magnetic field $\mathbf{B} = (B_x, B_y, B_z)$ pointing to an arbitrary direction. Schrödinger's equation is $-\sum_j t_{ij} e^{i\theta_{ij}} \psi_j = E \psi_i$, where ψ_i is the wave function at site i , the summation is over nearest-neighbor sites, and $\theta_{ij} = \frac{e}{\hbar} \int_j^i \mathbf{A} \cdot d\mathbf{l}$ is the Peierls phase with \mathbf{A} the vector potential, $\nabla \times \mathbf{A} = \mathbf{B}$. We consider a simple-cubic

lattice with a lattice constant a . Following Kunszt and Zee,⁸ we take a gauge $\mathbf{A} = (0, B_z x - (B_z B_x / B_y)(y - a/2), B_x y - B_y x)$, where z is cyclic. We can then write $\psi_{lmn} = e^{i\lambda_z n} F_{l,m}$, where l, m, n are site indices along x, y, z , respectively. Schrödinger's equation is then reduced to a two-dimensional tight-binding model,

$$\begin{aligned} & -t_x F_{l-1,m} - t_x F_{l+1,m} - t_y e^{2\pi i \phi_z [l - (\phi_x / \phi_y)(m-1)]} F_{l,m-1} \\ & - t_y e^{-2\pi i \phi_z [l - (\phi_x / \phi_y)m]} F_{l,m+1} \\ & - 2t_z \cos[2\pi(\phi_x l - \phi_y m) + \lambda_z] F_{l,m} = E F_{l,m}, \end{aligned} \quad (1)$$

where $t_i (i = x, y, z)$ is the transfer energy and $\phi_i = B_i a^2 / \phi_0$ with $\phi_0 \equiv h/e$ is respective number of flux quanta penetrating the facet of the unit cell normal to $\hat{\mathbf{e}}_i$. Here we consider rational fluxes,

$$(\phi_x, \phi_y, \phi_z) = \Phi \times (n_x, n_y, n_z), \quad \Phi = P/Q \quad (2)$$

with P, Q : integers and n_i 's are mutually prime integers. By introducing $j = n_y l - n_x m$, we can eliminate m from the phase factors (exponentials and the argument of cosine in Eq. (1)), so we can write $F_{j,m} = e^{i\lambda_y m} G_j$, where G is determined from a one-dimensional equation,

$$\begin{aligned} & -t_x G_{j+n_y} - t_x G_{j-n_y} \\ & - t_y e^{i[2\pi\Phi \frac{n_z}{n_y}(j+n_x) - \lambda_y]} G_{j+n_x} - t_y e^{-i(2\pi\Phi \frac{n_z}{n_y}j - \lambda_y)} G_{j-n_x} \\ & - 2t_z \cos(-2\pi\Phi j - \lambda_z) G_j = E G_j. \end{aligned} \quad (3)$$

Since the phase factors have a common periodicity $n_y Q$, we can apply the Bloch-Floquet theorem to have $G_{j+n_y Q} = e^{i\lambda_x n_y Q} G_j$, and the Hamiltonian is reduced to a $n_y Q \times n_y Q$ matrix.

III. ENERGY SPECTRA AND HALL CONDUCTIVITIES

Our aim is to search systematically for gapful spectra for the isotropic case with $t_x = t_y = t_z \equiv t$ and to determine the Hall conductivities for each energy gap. We have numerically solved Eq.(3) and obtained the energy spectra versus Φ . Fig. 1 shows the results for typical field directions: $(n_x, n_y, n_z) = (1, 2, 3), (1, 1, 2), (1, 1, 1)$, and $(0, 1, 2)$, which differ in symmetry. In each case we took 16 points for each of the Bloch wavenumbers $\lambda_x, \lambda_y, \lambda_z$.

We can immediately see that a series of gaps appear for $(n_x, n_y, n_z) = (1, 2, 3)$, while otherwise we have at most solitary gaps. From such results we have found that the spectrum has a series of gaps *when no two n_i 's coincide and $n_i \neq 0$* . So we can say that the gapful spectrum can be expected when \mathbf{B} points to general directions (i.e., off high-symmetry crystallographic axes). The gaps shrink when B is too small ($B a^2 / \phi_0 \ll 1$) obviously.

Now we proceed to the quantum Hall effect. As mentioned, E_F in an energy gap dictates³⁻⁵ quantized Hall conductivities,

$$(\sigma_{yz}, \sigma_{zx}, \sigma_{xy}) = -\frac{e^2}{ha}(m_x, m_y, m_z), \quad (4)$$

where m_i 's are integers satisfying a Diophantine's equation,

$$\nu_B = s + m_x \phi_x + m_y \phi_y + m_z \phi_z. \quad (5)$$

Here s is an integer, ν_B is the filling of the tight-binding band, and m_i 's assigned to each gap are topological invariants, i.e., they never change when external parameters (magnetic field, transfer energies, etc) are changed as long as the gap remains. So Eq.(5) tells us that, if we consider ν_B as a function of (ϕ_x, ϕ_y, ϕ_z) in a 4D parameter space $(\nu_B, \phi_x, \phi_y, \phi_z)$, the ν_B plotted along a gap assigned with (m_x, m_y, m_z) will form a '3D plane' having a gradient (m_x, m_y, m_z) in the 4D space.

In fact we can readily translate the E - Φ diagram in Fig. 1 to the ν_B - Φ diagram by counting the number of subbands below each value of E . There, the gradient $\partial \nu_B / \partial \Phi$ for each gap gives $m_x n_x + m_y n_y + m_z n_z$. We can then scan the direction of \mathbf{B} to determine all of m_x, m_y, m_z by keeping track of each gap in question, which is exactly how we have obtained the Hall integers here. The result is shown as triple integers in Fig. 1. We can see that the largest series of gaps have $(m_x, m_y, m_z) = (\pm 1, 0, 0), (0, \pm 1, 0)$ or $(0, 0, \pm 1)$, where only one of the Hall components is nonzero. This is strikingly new in that one and the same butterfly contains all the cases with $m_x \neq 0, m_y \neq 0, m_z \neq 0$, respectively, for a fixed direction of \mathbf{B} . This is in sharp contrast with the butterfly in the anisotropic case¹² where one component σ_{yz} is identically zero with x being the most conductive direction. Hence the versatile behavior of (m_x, m_y, m_z) may be regarded as a hallmark of the isotropic 3D QHE.

When the above condition is not satisfied (i.e., when two n_i 's coincide as in $(1, 1, 2)$ and $(1, 1, 1)$ or at least one $n_i = 0$ as in $(0, 1, 2)$), only solitary gaps or zero gaps (marked with dashed lines) appear. Hasegawa has shown for the case of $(1, 1, 1)$ that two bands touch where the energy dispersion is similar to those of a Dirac particle. We have similar band touching in Fig.1(b)(1, 1, 2) as well, for which a detailed calculation shows that the dispersion around the band touching is indeed linear in $\lambda_x, \lambda_y, \lambda_z$.

The reason for the band touching can be accounted for as follows. For $(n_x, n_y, n_z) = (1, 1, 2)$ (b), the gap for $(m_x, m_y, m_z) = (m, 0, 0)$ and that for $(0, m, 0)$ appear along the same line in the ν_B - Φ diagram, since the problem is symmetric against $x \leftrightarrow y$. If there were no band touching, the Hall integers for $(m, 0, 0)$ and $(0, m, 0)$ would become indefinite, which contradicts with the topological argument that we can always determine m_i 's uniquely when the gap is nonzero. So we can conclude that the band touching always occurs when two n_i 's coincide. This explains why the series of gaps seen in case (a) disappear as we make $n_x = n_y$ in (b) and then $n_x = n_y = n_z$ in (c). We still have to explain why the butterfly does not appear in case (d) with one of n_i 's

being zero. We address this question from a different viewpoint in the next section.

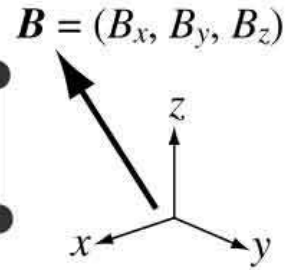
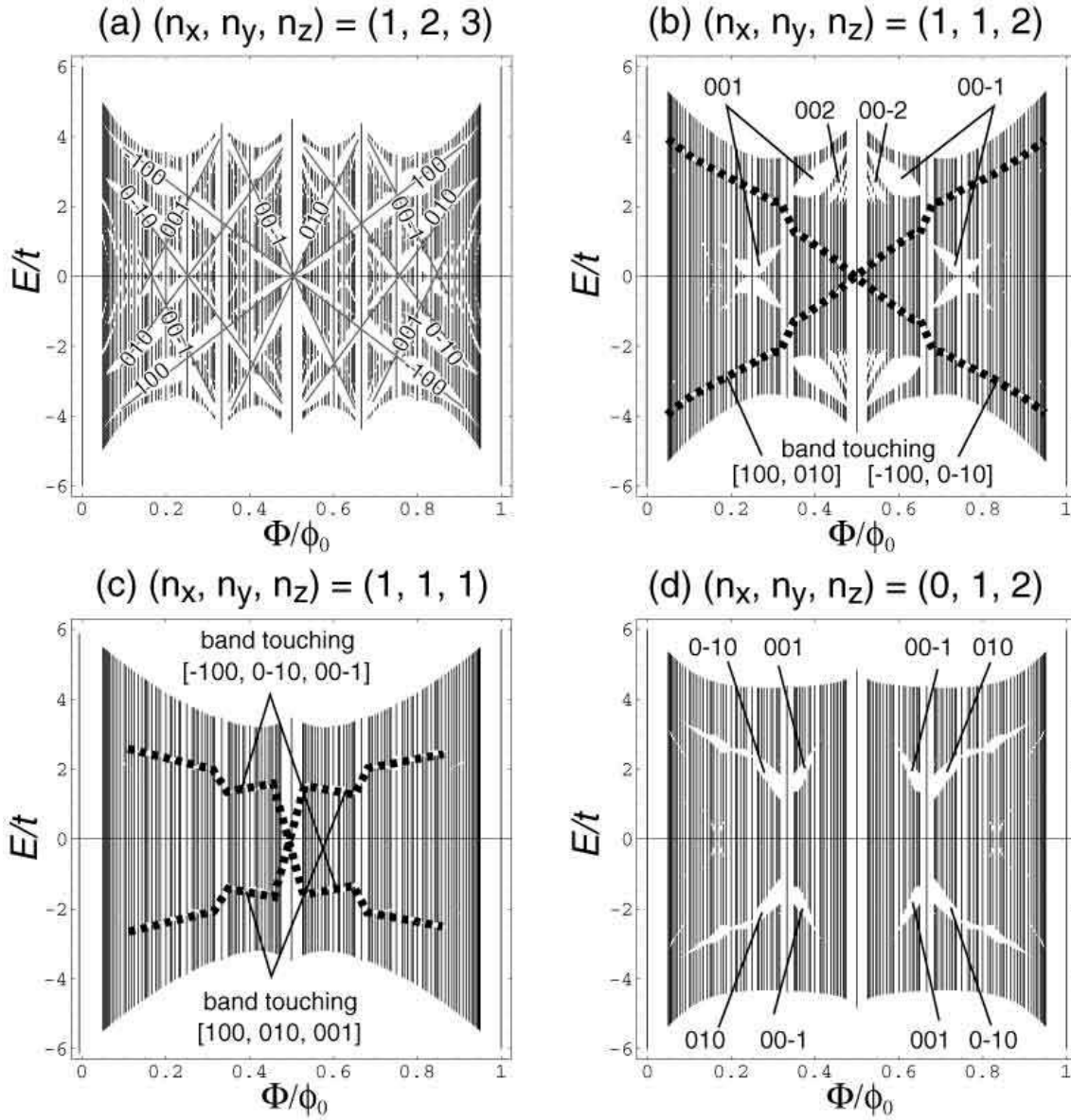


FIG. 1. Energy spectra for the isotropic simple-cubic lattice in the magnetic flux $(\phi_x, \phi_y, \phi_z) = \Phi \times (n_x, n_y, n_z)$ (as depicted in the inset). Each spectrum is plotted against Φ with the direction of \mathbf{B} fixed at (a) $(n_x, n_y, n_z) = (1, 2, 3)$, (b) $(1, 1, 2)$, (c) $(1, 1, 1)$, (d) $(0, 1, 2)$. Triple integers represent the Hall integers, $(\sigma_{xy}, \sigma_{yz}, \sigma_{zx})$ in units of $(-e^2/ha)$. Dashed lines in (b), (c) delineate the zero-gap.

IV. DUALITY FOR $B \leftrightarrow 1/B$

Electrons in magnetic fields are usually described in \mathbf{k} -space. A textbook example is the semiclassical picture, where an electron is treated as a classical particle driven in \mathbf{k} -space by a weak magnetic field. As B becomes stronger, the semiclassical orbits begin to be mixed and the picture breaks down. Actually this quantum mixing plays a critical role in opening the gaps and in quantization of the Hall conductivity as shown in the following.

We propose here that there exists a duality that relates a semiclassical picture in \mathbf{k} -space (weak- B case) to another semiclassical picture in the opposite limit of strong magnetic field, in which the *guiding center* of the cyclotron motion drifts along equipotential contours in the real space. Using a quantum mechanical mapping from the weak- B case to the strong- B case (where B translates into $1/B$), we are able to discuss the mixing of semiclassical orbits in our problem (3D lattice in \mathbf{B}) in a clear cut.

Let us derive the duality in 2D and then extend it to 3D. We consider a 2D Bloch electron with the dispersion $\varepsilon(k_x, k_y)$ in a magnetic field B perpendicular to the plane. If we define the dynamical wavevector $\mathbf{K} \equiv \mathbf{k} + (e/\hbar)\mathbf{A}$, the Hamiltonian in k -space is written as

$$H = \varepsilon(K_x, K_y), \\ [K_x, K_y] = -ieB/\hbar. \quad (6)$$

This is an exact quantum equation except that we have neglected the inter-band mixing due to the magnetic field, which is allowed when the periodic potential is strong enough (or the magnetic field is weak enough). The equation reduces to the semiclassical one in the limit $eB/\hbar \rightarrow 0$.

If we consider another 2D system in a magnetic field B with a periodic potential $V(\mathbf{r})$ with $\mathbf{r} \equiv (x, y)$, the Hamiltonian in real space is written as

$$H = \frac{1}{2m}(\mathbf{p} + e\mathbf{A})^2 + V(\mathbf{r}) \\ = \frac{1}{2m}\mathbf{\Pi}^2 + V\left(\mathbf{R} - \frac{1}{eB}\hat{\mathbf{e}}_z \times \mathbf{\Pi}\right), \quad (7)$$

where $\mathbf{\Pi} \equiv \mathbf{p} + e\mathbf{A}$ and $\mathbf{R} = \mathbf{r} - \boldsymbol{\xi}$ is the cyclotron-motion guiding center with the relative coordinate given as $\boldsymbol{\xi} = -(1/eB)\hat{\mathbf{e}}_z \times \mathbf{\Pi}$.

When the magnetic field is strong enough (or the potential V is weak enough) so that (i) the magnetic length $l = \sqrt{\hbar/(eB)}$ is much shorter than the length scale over which V varies, and that (ii) the different Landau levels are not mixed, we can consider $\mathbf{\Pi}$ to be frozen. More precisely, the kinetic energy (the first term in Eq.(7)) reduces to a constant from (ii), while the second term can be approximated as $V(\mathbf{R})$ from (i). The Hamiltonian then becomes, up to a constant,

$$H \approx V(X, Y), \\ [X, Y] = i\hbar/(eB). \quad (8)$$

We can see that Eqs. (6) and (8) are identical if we translate as

$$\mathbf{K} \leftrightarrow \mathbf{X}, \quad \varepsilon \leftrightarrow V, \quad \frac{eB}{\hbar} \leftrightarrow \frac{\hbar}{eB}. \quad (9)$$

So we can see that there exists a duality between the 2D system with a strong periodic potential in a weak B (one band tight-binding model) and the 2D system with a weak periodic potential in a strong field (one Landau level approximation). For the Landau level in the latter case we expect that the duality holds best in the lowest Landau level, since the wavefunction is most localized in that level to make Eq. (8) valid.

The duality introduced here provides a physical basis for Hofstadter's observation¹ on the mapping between the tight-binding and weak-potential systems⁹ for the square lattice, and also generally applicable to any 2D lattices, or, remarkably, 3D cases as well as we shall see below. Another duality is found by Ishikawa *et al*³, which is distinct from ours in that one Landau level is mapped to one Landau level in the latter while one Landau level is mapped to one Bloch band in the present case.

Now we apply the duality to 3D systems, which enables us to have a fresh look at the 3D QHE. We take the Bloch electron with the dispersion $\varepsilon(k_x, k_y, k_z)$ in a magnetic field $\mathbf{B} = (B_x, B_y, B_z)$. Let us again denote the direction of \mathbf{B} as $\mathbf{n} \equiv (n_x, n_y, n_z)$ whose components will be assigned a set of integers. We set a new frame (x', y', z') in which the magnetic field point to $(0, 0, 1)$. If we take the vector potential \mathbf{A} with $A_z = 0$, we have

$$H = \varepsilon(K_{x'}, K_{y'}, k_{z'}), \quad (10)$$

where $K_i = k_i + (e/\hbar)A_i$ ($i = x', y'$) with $[K_{x'}, K_{y'}] = -ieB/\hbar$ while $k_{z'}$ remains a quantum number. We can thus apply the above duality to this system, which implies that the 3D system can be mapped to a system in a fictitious 2D space $(K_{x'}, K_{y'})$ with a potential $\varepsilon(K_{x'}, K_{y'}, k_{z'})$ in a fictitious magnetic field B^* with $\hbar/(eB^*) = eB/\hbar$. The mapping is valid for a large B^* , i.e., a small B . The fictitious potential is a cross section of the 3D dispersion incised at $k_{z'}$ by a plane perpendicular to \mathbf{B} . As we shift $k_{z'}$, the 2D potential changes accordingly, and the spectrum is determined by taking all the possible values of $k_{z'}$.

We take a cubic dispersion,

$$\varepsilon(k_x, k_y, k_z) = -t_x \cos k_x a - t_y \cos k_y a - t_z \cos k_z a, \quad (11)$$

which is written in the new frame as,

$$\varepsilon(k_{x'}, k_{y'}, k_{z'}) = -t_x \cos[\mathbf{G}_x \cdot \mathbf{k}_\perp + (n_x/n)k_{z'}a] \\ - t_y \cos[\mathbf{G}_y \cdot \mathbf{k}_\perp + (n_y/n)k_{z'}a] \\ - t_z \cos[\mathbf{G}_z \cdot \mathbf{k}_\perp + (n_z/n)k_{z'}a], \quad (12)$$

where $\mathbf{k}_\perp \equiv (k_x', k_y')$, $n = \sqrt{n_x^2 + n_y^2 + n_z^2}$ and

$$\begin{aligned}\mathbf{G}_x &= \tilde{a}(n_z n_x/n, -n_y), \\ \mathbf{G}_y &= \tilde{a}(n_y n_z/n, n_x), \\ \mathbf{G}_z &= \tilde{a}(-(n_x^2 + n_y^2)/n, 0),\end{aligned}\quad (13)$$

with $\tilde{a} \equiv a/\sqrt{n_x^2 + n_y^2}$. Now we can see that our 3D problem is reduced to a fictitious 2D system having three periods [while the Hofstadter problem (2D Bloch system in B) is reduced to a 1D system having two periods]. The Hamiltonian for the fictitious 2D system is

$$H = \frac{1}{2m}(\mathbf{p}^* + e\mathbf{A}^*)^2 + \varepsilon(K_x', K_y', k_{z'}), \quad (14)$$

where $\mathbf{p}^* = (\partial/\partial K_x', \partial/\partial K_y')$ and \mathbf{A}^* is a vector potential for the fictitious magnetic field $(0, 0, B^*)$. Since we assume a large B^* , Schrödinger's equation can be written within the basis for the lowest Landau level, which reads, after a certain phase transformation,

$$\begin{aligned}-\tilde{t}_x \Psi_{j+n_y} - \tilde{t}_x \Psi_{j-n_y} - \tilde{t}_y e^{i[2\pi\Phi\frac{n_z}{n_y}(j+\frac{n_x}{2})-\lambda_y]} \Psi_{j+n_x} \\ - \tilde{t}_y e^{-i[2\pi\Phi\frac{n_z}{n_y}(j-\frac{n_x}{2})-\lambda_y]} \Psi_{j-n_x} \\ - 2\tilde{t}_z \cos(-2\pi\Phi j - \lambda_z) \Psi_j = E \Psi_j.\end{aligned}\quad (15)$$

Here the hopping parameters are

$$\tilde{t}_i = t_i e^{-G_i^2 l^{*2}/4}, \quad (16)$$

$l^* \equiv \sqrt{\hbar/(eB^*)}$ is the fictitious magnetic length, and λ_y, λ_z are given by

$$\begin{aligned}\lambda_y &= -\Phi \frac{n_z}{n_y} \alpha + \frac{n_x^2 + n_y^2}{nn_y} k_{z'} a \\ \lambda_z &= -\Phi \alpha + \frac{n_z}{n} k_{z'} a,\end{aligned}\quad (17)$$

where α labels the wavefunction in the lowest Landau level. Now the duality implies that Eq.(15) should reduce to Eq.(3) in the strong B^* limit (i.e., weak B limit), since l^* should become smaller than the potential range $1/G_i$ so that \tilde{t}_i tends to t_i .

V. INTERPRETATION OF THE 3D QHE FROM THE DUALITY

The mapping via the duality enables us to see how the total spectrum comes from dispersion relations versus $k_{z'}$, which helps intuitively understanding how the energy gaps open and how the Hall conductivities are quantized. Since the mapping is limited to the weak- B case, we examine the situation where the gaps begin to open in the quantum regime approached from the semiclassical one. We show in Fig.2 the band structure versus $k_{z'}$ for the fictitious system (Eq.(15)), along with the fictitious potential $\varepsilon(K_x', K_y', k_{z'})$ for fixed values of $k_{z'}$.

Let us first look at how the energy spectra can have gaps for general directions of $\mathbf{n}[\propto (1, 2, 3)$ in Fig.2(a)]. ε accommodates closed orbits around its peaks and dips in the “semiclassical picture” in the language for the weak- B (strong- B^*) case, where the area enclosed by each orbit must be a multiple of $2\pi/l^2$. So the different wells have different sets of discrete levels, where each level moves on the energy axis as $k_{z'}$ is changed, since ε changes its form with $k_{z'}$. When the levels belonging to the wells adjacent in $K_x' K_y'$ -space coincide, the states will strongly resonate quantum-mechanically and an energy gap will arise. In Fig.2(a), we show the case where the gaps begin to open with $(\phi_x, \phi_y, \phi_z) = (1/9)(1, 2, 3)$, for which the strong mixing of orbits is seen to result in significant level repulsions. We attach for comparison the result for an almost semiclassical case when the magnetic field, $(\phi_x, \phi_y, \phi_z) = (1/45)(1, 2, 3)$, is so small that the mixing is weak and the level repulsion is almost negligible except for the middle of the total band.

In terms of the semi-classical orbits, the change in $k_{z'}$ causes the orbits to hop to adjacent positions at every resonance as shown in Fig.2. A virtue of this picture is that *the distance and the direction of the hopping exactly indicates the Hall integers*, as shown in the following. If we apply an infinitesimal electric field \mathbf{E} to the system, $k_{z'}$ is dragged adiabatically according to an equation, $\hbar(dk_{z'}/dt) = -eE_{z'}$, where $\mathbf{E}_{z'}$ is the component parallel to z' . After $k_{z'}$ is changed by $\delta k_{z'} \equiv 2\pi/(an)$ (the period with which the spectrum repeats itself), every state must come back to the equivalent position in the reciprocal unit cell. Note here that the cell boundaries (represented in Fig.2 as white lines) also move as $k_{z'}$ is changed, since the Brillouin zone boundaries are oblique with $z' \parallel \mathbf{B}$. The increment in k -space, $\delta\mathbf{K} = (\delta K_x', \delta K_y', \delta k_{z'})$, with which the orbit is shifted over the one period satisfies

$$\begin{aligned}\delta\mathbf{K} &= \mp \frac{2\pi}{a} \delta\mathbf{m}, \\ \delta\mathbf{m} &= \delta m_x \hat{\mathbf{e}}_x + \delta m_y \hat{\mathbf{e}}_y + \delta m_z \hat{\mathbf{e}}_z,\end{aligned}\quad (18)$$

where $-$ and $+$ correspond to positive and negative $E_{z'}$, respectively, and δm_i 's are integers assigned to each subband. The integers satisfy a relation $\delta\mathbf{m} \cdot \mathbf{n} = 1$, since $\delta k_{z'} = 2\pi/(an)$. We can immediately translate $\delta\mathbf{K}$ into the motion in the real space normal to z' using the relationship between the relative coordinate $\boldsymbol{\xi}$ and the dynamical wavenumber \mathbf{K} ,

$$\delta\boldsymbol{\xi} = -\frac{\hbar}{eB} \hat{\mathbf{e}}_{z'} \times \delta\mathbf{K}. \quad (19)$$

Since the system has no dissipation as long as E_F is in a gap, $\mathbf{E}_{z'}$ should cause no net current along z' . Therefore the velocity averaged over one period driven by $\mathbf{E}_{z'}$ is just the ratio of $\delta\boldsymbol{\xi}$ and the one period ($= \delta k_{z'}/(e|E_{z'}|/\hbar)$), which leads to $\mathbf{v} = (n/B)\mathbf{E}_{z'} \times \delta\mathbf{m}$. The Hall current due to $\mathbf{E}_{z'}$ is calculated as

$$\mathbf{j} = -\rho e \mathbf{v} = \frac{e^2}{ha} \delta \mathbf{m} \times \mathbf{E}_{z'}, \quad (20)$$

where $\rho = eB/(ahn)$ is the density of states per subband and per unit volume. From this expression we can write the Hall tensor as $\hat{\sigma}_\perp = -(e^2/ha) \delta \mathbf{m}_\perp$, where $\sigma_{ij} \equiv \epsilon_{ijk} \hat{\sigma}_k$, and \perp represents the component normal to z' . On the other hand, the normal component of the electric field, \mathbf{E}_\perp causes a classical drift in the direction normal to z' with the velocity $\mathbf{v} = (\mathbf{E}_\perp \times \mathbf{B})/B^2 = (n/B) \mathbf{E}_\perp \times \delta \mathbf{m}$, which immediately leads to $\hat{\sigma}_{z'} = -(e^2/ha) \delta m_{z'}$. Combining the two, we finally obtain the quantized Hall conductivity carried by the corresponding subband,

$$\hat{\sigma} = -(e^2/ha) \delta \mathbf{m}. \quad (21)$$

We have thus derived the quantization of the 3D Hall conductivity from the \mathbf{k} -space hopping, as an approach alternative to the usual Kubo formula. The problem of the transport in adiabatically varying potentials (so-called Thouless pumping) was first considered by Thouless¹⁴ for one-dimensional case. He showed that the 2D QHE in periodic potentials may be understood in terms of a fictitious 1D system having two periodic potentials that slide adiabatically with each other. The discussion we have given here to describe the 3D QHE may be regarded as a two-dimensional version of the Thouless pumping.

We can actually identify the Hall integers δm_i for each subband by keeping track of the motion of the orbits with $k_{z'}$. Figure 2(a) typically depicts how a state in the first band moves by $(1,0,0)$, by which we mean the state jumps once across a reciprocal cell boundary normal to k_x (whose intersection is shown as one of the white lines in Fig.2) but not across k_y or k_z . The state in the second band moves by $(-1,1,0)$. These triple numbers are the very Hall integers, $(\delta m_x, \delta m_y, \delta m_z)$, carried by each subband (not to be confused with the total Hall integer), and are in accordance with the small Φ region in Fig.1(a).

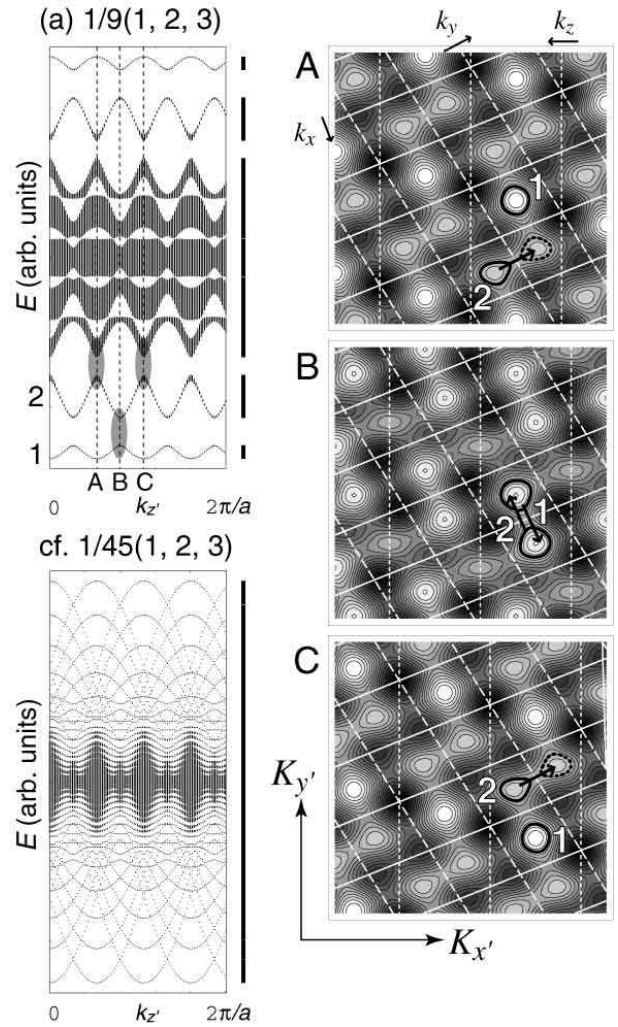
We can now comment on the relation with the usual treatment of 3D QHE³⁻⁵. By summing up $\delta \mathbf{m} \cdot \mathbf{n} = 1$ over the occupied subbands, we have $\mathbf{m} \cdot \mathbf{n} = r$, where r is the number of occupied subbands and \mathbf{m} is the summation of $\delta \mathbf{m}$ over them. Since r is related to the filling of the tight-binding band in $\nu_B = r \times \rho/(1/a^3)$, we obtain

$$\nu_B = m_x \phi_x + m_y \phi_y + m_z \phi_z, \quad (22)$$

which coincides with the Diophantine equation (5) for $s = 0$. This means that in our picture above, only the gaps with $s = 0$ are taken into account while the rest are neglected. We can actually show that the gap associated with $s \neq 0$ only occurs, when the magnetic field is weak ($\Phi \ll 1$), as a small gap between very dispersive bands (versus $k_{z'}$), so that the gap vanishes in the spectrum. Weak field regime is exactly the situation considered here, since we are approaching to the quantum regime from the semiclassical one. The discussion here is for the lower half of the tight-binding band, while we can make a similar argument for the upper half in terms

of hole orbits, which can be obtained as an electron-hole transformation (on the ν_B - Φ diagram), which in turn corresponds to $s = 0 \rightarrow 1$ in the Diophantine equation.

The mapped picture also gives an intuitive explanation why we have so few gaps for the symmetric case Fig.2(b),(c), and zero-component case (d). When two components in \mathbf{n} coincide as in Fig.2(b) with $\mathbf{n} \propto (1, 1, 2)$, while two levels cross (for the value of $k_{z'}$ labeled as B), a gap does not arise because the couplings along k_x and k_y occur symmetrically (in a zigzag fashion), so that the bands do not split, which is exactly the band touching discussed in Sec. III. When the symmetry is even higher with $\mathbf{n} \propto (1, 1, 1)$ in Fig.2(c), couplings along k_x , k_y and k_z all become symmetric and the band touching occurs at every energy crossing. If \mathbf{n} contains a zero component as in (d), two of the plane waves for ε become parallel and the wells having the same depth become connected along the perpendicular direction. This results in a strong mixing between the states along that trough direction, so that the minibands for each value of $k_{z'}$ become wider. So, while the energy gap does arise when the energies of the adjacent troughs coincide, these gaps tend to be overlapped in energy by other, wide bands.



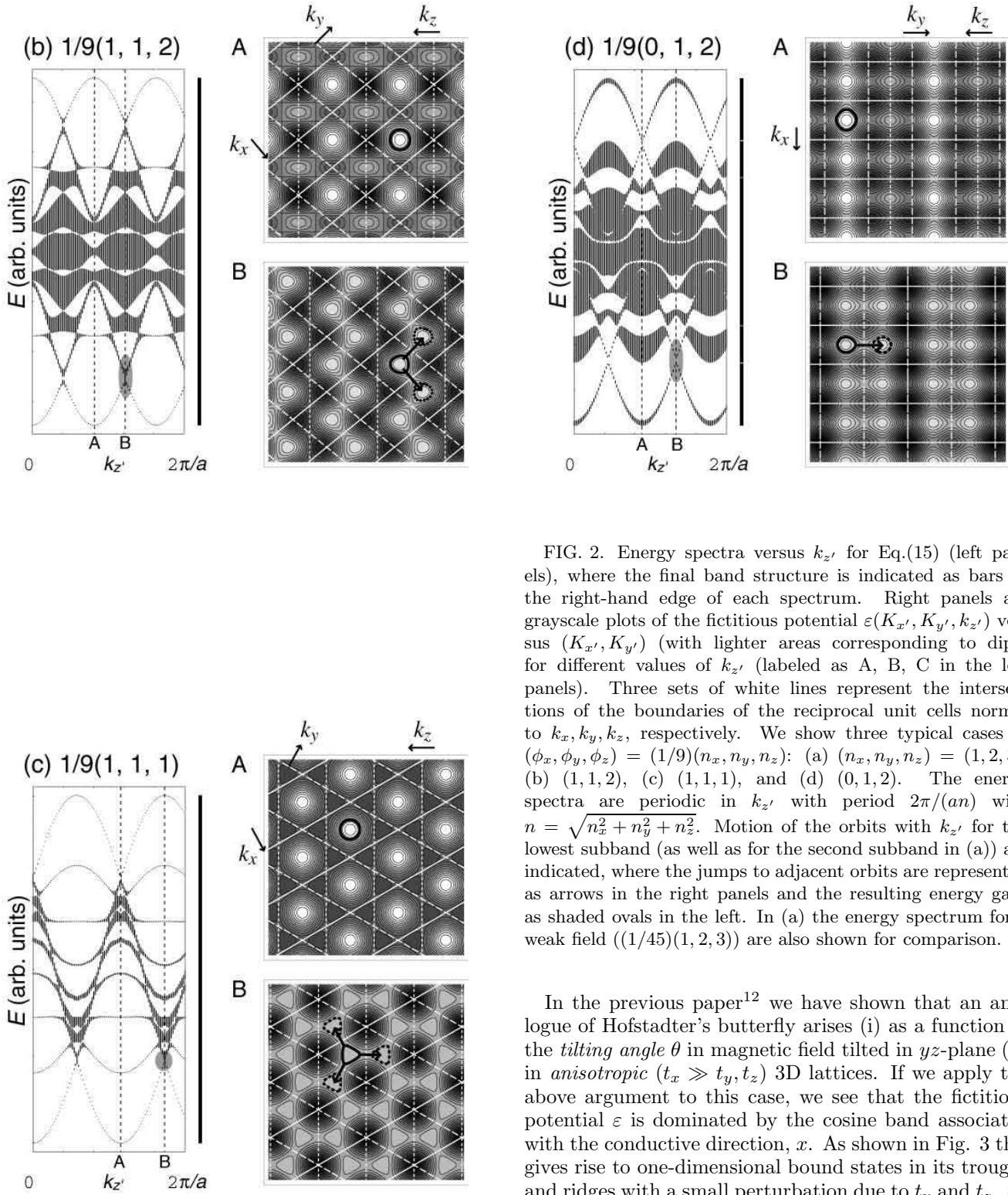


FIG. 2. Energy spectra versus k_z' for Eq.(15) (left panels), where the final band structure is indicated as bars at the right-hand edge of each spectrum. Right panels are grayscale plots of the fictitious potential $\varepsilon(K_x', K_y', k_z')$ versus (K_x', K_y') (with lighter areas corresponding to dips) for different values of k_z' (labeled as A, B, C in the left panels). Three sets of white lines represent the intersections of the boundaries of the reciprocal unit cells normal to k_x, k_y, k_z , respectively. We show three typical cases of $(\phi_x, \phi_y, \phi_z) = (1/9)(n_x, n_y, n_z)$: (a) $(n_x, n_y, n_z) = (1, 2, 3)$, (b) $(1, 1, 2)$, (c) $(1, 1, 1)$, and (d) $(0, 1, 2)$. The energy spectra are periodic in k_z' with period $2\pi/(an)$ with $n = \sqrt{n_x^2 + n_y^2 + n_z^2}$. Motion of the orbits with k_z' for the lowest subband (as well as for the second subband in (a)) are indicated, where the jumps to adjacent orbits are represented as arrows in the right panels and the resulting energy gaps as shaded ovals in the left. In (a) the energy spectrum for a weak field $((1/45)(1, 2, 3))$ are also shown for comparison.

In the previous paper¹² we have shown that an analogue of Hofstadter's butterfly arises (i) as a function of the *tilting angle* θ in magnetic field tilted in yz -plane (ii) in *anisotropic* ($t_x \gg t_y, t_z$) 3D lattices. If we apply the above argument to this case, we see that the fictitious potential ε is dominated by the cosine band associated with the conductive direction, x . As shown in Fig. 3 this gives rise to one-dimensional bound states in its troughs and ridges with a small perturbation due to t_y and t_z . So the system can be regarded as an array of independent chains with two periods, which is described by a Harper's equation for the 2D Hofstadter's problem, and thus we can understand why the anisotropic case can have many gaps around the top and bottom of the band as seen in Fig. 3, while one component σ_{yz} is fixed to 0 unlike the isotropic case.

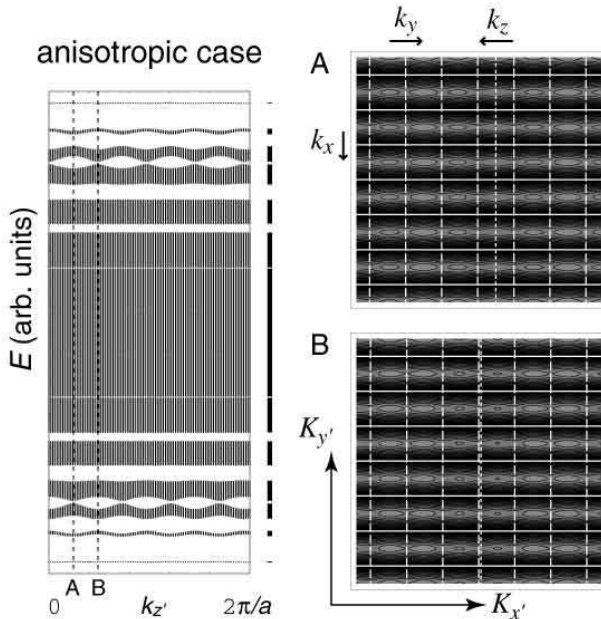


FIG. 3. A plot similar to Fig.2 for an anisotropic 3D system with $(t_x, t_y, t_z) = (1.0, 0.1, 0.1)$ for $(\phi_x, \phi_y, \phi_z) = (1/15)(0, 1, 4)$. The contours highlight the troughs.

VI. DUAL HALL CONDUCTIVITY

We have just shown that two different systems related by the duality have similar energy spectra. It would be then interesting to see how the Hall conductivities are related between them for the corresponding energy gaps. For the 2D case, Thouless *et al*² have shown the relationship between the Hall integers in the tight-binding and in the strong-field limits. Here we first review this in the context of our duality before moving on to the 3D case. Diophantine's equation for an energy gap in the 2D tight-binding case (a 2D version of Eq.5) is

$$\nu_B = s + t\phi, \quad (23)$$

where s, t are integers, ν_B the tight-binding band filling, and ϕ the number of fluxes penetrating the 2D unit cell. The equation for the corresponding gap in the 2D strong-field case is written with the same s, t as

$$\nu_L = s + t(1/\phi), \quad (24)$$

where ν_L is the Landau-level filling factor, i.e., the fraction of the filled states in the lowest Landau level, and ϕ is replaced with $1/\phi$ according to the duality (Eq.9). From the relation $\nu_L = \nu_B/\phi$, we can translate Eq.(24) into

$$\nu_B = s\phi + t. \quad (25)$$

$$\sigma_{xy} = -\frac{e^2}{h} \frac{\partial \nu_B}{\partial \phi}, \quad (26)$$

indeed dictates that the Hall conductivity is the gradient in ν_B - ϕ diagram, which gives $-(e^2/h)t$ in the former case $-(e^2/h)s$ in the latter.

This results can be readily extend to the 3D case. Namely, if we take an energy gap in the 3D system with $(\sigma_{yz}, \sigma_{zx}, \sigma_{xy}) = -\frac{e^2}{\hbar a}(m_x, m_y, m_z)$, the Hall conductivity in the corresponding 2D system becomes $-(e^2/h)s$, where m_i and s are related via Eq.(5).

VII. EXPERIMENTAL FEASIBILITY

Let us comment on the magnitude of the magnetic field required to observe the energy gaps in 3D systems. For that it is essential that the coupling between the semiclassical orbits in the different wells exists. For the isotropic crystals considered here, the area enclosed by the semiclassical orbit in \mathbf{k} -space should be of the order of the typical well area, $2\pi/l^2 \sim (2\pi/a)^2$, which is simply $Ba^2/\phi_0 \sim 1$. The situation is the same as in the 2D Hofstadter problem, so the required field for atomic lattice constants is huge ($B \sim 10^5$ T for $a = 2$ Å). If we consider systems with larger unit cells, as in solid fullerene or zeolites with $a = 10$ Å, the required B is reduced to 10^3 T but still large. In the anisotropic case discussed in Ref.¹², by contrast, the required is much less stringent. This is because the typical well area is $(2\pi/a)d$ with d being the typical valley width, so the condition relaxes to $2\pi/l^2 \sim (2\pi/a)d$, which can be made as small as one wishes by increasing the anisotropy (since $t_y, t_z \rightarrow 0$ leads to $d \rightarrow 0$), although the scale of the energy gap shrinks. So it is a trade-off between large B required with large energy gaps (isotropic case) and smaller B suffices with small gaps (anisotropic).

Another point is that a real 3D sample has always surfaces. Halperin and the present authors have shown in general that the 3D integer QHE should accompany quantized *wrapping* current, whose intensity and direction are dictated by the quantum Hall integers¹⁵. This should apply to the present case of isotropic QHE.

VIII. CONCLUSION

We have investigated the energy spectra in the isotropic 3D lattice in magnetic fields applied in arbitrary directions, for which we have shown that the energy gaps arise unless the magnetic field points to high-symmetry directions. We have also calculated the quantum Hall integers. In the latter part of the paper we have introduced a duality that relates $B \leftrightarrow 1/B$ (i.e., guiding center picture in strong B and semiclassical picture in weak B) for

the present 3D problem, which gives the graphic explanation of the quantization of the Hall conductivity in 3D and the condition for the butterfly spectrum.

M.K. would like to thank the JSPS for a financial support.

⁵ M. Kohmoto, B. I. Halperin, and Y. Wu, Phys. Rev. B **45**, 13488 (1992).
⁶ The 3D topological invariants are later interpreted as Berry's phase by J. Goryo and M. Kohmoto, J. Phys. Soc. Jpn. **71**, 1403 (2002).
⁷ Y. Hasegawa, J. Phys. Soc. Jpn. **59**, 4384 (1990); **61**, 1657 (1991).
⁸ Z. Kunszt and A. Zee, Phys. Rev. B **44**, 6842 (1991).
⁹ A. Rauh, Phys. Status Solidi B **69**, K9 (1975).
¹⁰ A. Widom, Phys. Lett. **90A**, 474 (1982).
¹¹ P. Středa, J. Phys. C **15**, L718 (1982).
¹² M. Koshino, H. Aoki, K. Kuroki, S. Kagoshima, and T. Osada, Phys. Rev. Lett. **86**, 1062 (2001).
¹³ K. Ishikawa, N. Maeda, T. Ochiai, and H. Suzuki, Phys. Rev. B **58**, 1088 (1998).
¹⁴ D. J. Thouless, Phys. Rev. B **27**, 6083 (1983).
¹⁵ Mikito Koshino, Hideo Aoki, Bertrand I. Halperin, Phys. Rev. B **66**, 081301(R) (2002).